FEBS Letters 530 (2002) 174–180 FEBS 26637

Yeast Mon1p/Aut12p functions in vacuolar fusion of autophagosomes and cvt-vesicles

Khuyen Meiling-Wesse[a], Henning Barth[a], Christiane Voss[a], Gunilla Barmark[b], Eva Murén[b], Hans Ronne[b], Michael Thumm[a,*]

[a] *Institute of Biochemistry, University of Stuttgart, Pfaffenwaldring 55, 70569 Stuttgart, Germany*
[b] *Department of Plant Biology, Uppsala Genetic Center, Swedish University of Agricultural Sciences, Box 7080, S-750 07 Uppsala, Sweden*

Received 19 August 2002; accepted 15 September 2002

First published online 30 September 2002

Edited by Horst Feldmann

Abstract Here we identify Mon1p as being essential for the cvt-pathway and autophagy. Thus, *mon1*Δ cells are impaired in proaminopeptidase I maturation and homozygous diploid *mon1*Δ cells do not sporulate. Quantitative autophagy measurements suggest a complete autophagy block. The autophagosomal marker protein GFP-Aut7p accumulates in *mon1*Δ cells at punctate structures outside the vacuole. Furthermore, proaminopeptidase I accumulates in *mon1*Δ cells in a proteinase-protected form. Our data demonstrate that *mon1*Δ cells are defective in the fusion of cvt-vesicles and autophagosomes with the vacuole. Consistent with this, GFP-Mon1p localizes to the cytosol and to punctate structures within the cytosol.

Key words: Ypt7; Ccz1; Vacuolar fusion; Autophagy; Vesicle docking; Yeast

1. Introduction

The *MON1* gene was initially identified in a screen for knockout mutants that cause hypersensitivity against the drugs monensin and brefeldin A [1]. These drugs are supposed to interfere with intracellular protein transport processes. Consistently, *MON1* also appeared in a genomic screen for mutants that secrete the vacuolar CPY [2]. It was further shown that *mon1*Δ cells have fragmented vacuoles and that they are defective in the maturation of both vacuolar carboxypeptidase Y and proteinase A. A retardation of vacuolar alkaline phosphatase maturation was also observed. These studies suggest a function of Mon1p during vacuolar protein sorting, but did not reveal where Mon1p functions within this pathway.

We are interested in the molecular mechanisms of the autophagic protein transport in *Saccharomyces cerevisiae*. Autophagy unspecifically delivers parts of the cytoplasm for degradation to the vacuole [3,4]. This starvation-induced recycling pathway assures cell survival during starvation. Mechanistically, autophagy starts at the preautophagosomal (perivacuolar) structure [5,6], where double membrane transport vesicles (autophagosomes) are formed [7]. Autophagosomes can enclose not only cytosolic material but also organelles, such as mitochondria, parts of the ER and peroxisomes. After fusion of the autophagosomal outer membrane with the vacuole, membrane-enclosed autophagic bodies are released into the vacuole. Vacuolar breakdown of autophagic bodies and their contents depends on vacuolar proteinase B [8], Aut4p [9] and the putative lipase Cvt17/Aut5p [10,11]. During starvation proaminopeptidase I is selectively targeted via autophagy to the vacuole, where mature aminopeptidase I is formed. Under nutrient-rich conditions, however, proaminopeptidase I transport is taken over by the cvt-pathway. The cvt-pathway is morphologically very similar to autophagy, but its transport intermediates (cvt-vesicles) are smaller than autophagosomes and exclude cytosol [12]. Autophagy proteins are to a large extent also involved in the cvt-pathway.

Here we identify Mon1p as a novel component essential for both the cvt-pathway and autophagy. Thus fluorescence microscopy using the autophagosomal marker protein GFP-Aut7p together with data on the accumulation of proaminopeptidase I in a proteinase K-protected form reveal that *mon1*Δ cells have a defect in the vacuolar fusion of cvt-vesicles and autophagosomes.

2. Materials and methods

2.1. Strains, media, antibodies and reagents

Standard media were used [13]. Starvation medium: 1% potassium acetate or SD–N (0.17% yeast nitrogen base without amino acids and ammonium sulfate, 2% glucose).

Antibodies: anti-green fluorescent protein (GFP), anti-3-phosphoglycerate kinase (PGK), and anti-carboxypeptidase Y (CPY) (Molecular Probes, Leiden, The Netherlands), horseradish peroxidase (HRPO)-conjugated goat anti-rabbit (Medac, Hamburg, Germany) and HRPO-conjugated goat anti-mouse (Dianova, Hamburg, Germany), anti-proaminopeptidase I [14].

Chemicals: oxalyticase (Enzogenetics, Corvallis, OR, USA), phenylmethylsulfonylfluoride (PMSF) (Sigma, Deisenhofen, Germany), PVDF-membrane (Bio-Rad, Hercules, CA, USA), oligonucleotides (MWG Biotec, Ebersberg, Germany), restriction enzymes (Roche, Mannheim, Germany). Other analytical grade chemicals were from Sigma (Munich, Germany) or Merck (Darmstadt, Germany). Immunoblots were developed with an ECL detection kit (Amersham, Braunschweig, Germany).

2.2. MON1 and PHO8 chromosomal deletion

A PCR fragment conferring kanamycin resistance was created with plasmid pUG6 [19] and the primers: S-MON1 TCTATCAAAGTACACAAACGTAGAATCAGTACATCGGAACT and AS-MON1 AATAACCTCCCTGTCACAAGTTAAAACACGGCCCCATCAC. This fragment was used to chromosomally delete *MON1* in WCG4a, yielding YKMW2 (Table 1). Gene replacement was confirmed by

*Corresponding author. Fax: (49)-711-685 4392.
E-mail address: thumm@po.uni-stuttgart.de (M. Thumm).

0014-5793/02/$22.00
PII: S0014-5793(02)03456-7

Southern (not shown). YUE63, YUE66, YKMW22, YKMW20 were created using the *pho8Δ::LEU2* deletion plasmid pGF10 [20].

2.3. Determination of sporulation frequency

Stationary phase homozygous diploid cells were shifted to 1% potassium-acetate. After 3, 6 and 10 days at room temperature the number of sporulated cells was counted and expressed as a percentage of the total cells. In the genetic background used (BY4743, Euroscarf, Frankfurt, Germany), dyads are often seen in addition to tetrads. Both were counted as sporulated cells.

2.4. Alkaline Phosphatase Assay

The *pho8Δ::LEU2* deletion strains were transformed with the Pho8Δ60-expression plasmid pCC5 [21]. Enzymatic activity was measured as described [22] with the following modifications. Logarithmically grown cells were washed with water and resuspended in SD–N medium. One OD_{600} unit of cells was harvested at each time point and washed once with water. The cells were then suspended in 0.2 ml of assay buffer (250 mM Tris–HCl, pH 9.0, 10 mM $MgSO_4$, 10 μM $ZnSO_4$) and disrupted by vortexing with glass beads. After centrifugation, 50 μl of the supernatant was added to 0.5 ml of assay buffer and 50 μl of 55 mM α-naphtylphosphate. After incubation for 15 min at 30°C, 0.5 ml of 2 M glycine-NaOH (pH 11.0) was added to stop the reaction. Fluorescence intensity was measured with excitation at 345 nm and emission at 472 nm. Protein concentration was determined with the BCA method (Pierce, Rockford, IL, USA).

2.5. Proteinase K protection

Proteinase protection was done according to [23] with the following modifications. 40 OD_{600} units of stationary phase or starved cells were harvested, washed twice with water and incubated for 15 min in 20 mM DTT containing 100 mM Tris–HCl buffer, pH 9.4. The cells were then resuspended in 1 M sorbitol, 50 mM sodium phosphate buffer pH 7.4 containing 50 μg/ml oxalyticase, and spheroplasted at 30°C for 30 min. The spheroplasts were hypotonically lysed by resuspending in PS200 (20 mM potassium-PIPES, 200 mM Sorbitol, pH 6.8 with 5 mM $MgCl_2$). Cell debris was removed by repeated centrifugation and the supernatant divided into three 300-μl fractions. 300 μl PS200, PS200 with 50 μg/ml Proteinase K, and PS200 with 50 μg/ml Proteinase K and 0.4% Triton X-100 were added to each fraction, respectively. After 15 min on ice, digestion was stopped through trichloroacetic acid precipitation.

2.6. GFP-Aut7p degradation

Mid-log cells grown in SMD were starved in SD–N. One OD_{600} unit of cells was hourly harvested for 4 h. The samples were processed for immunoblotting. Plasmid pGFP-AUT7 is described in [5].

2.7. Generation and localization of GFP-Mon1

MON1 was amplified from BY4742 (Euroscarf, http://www.uni-frankfurt.de/fb15/mikro/euroscarf/) genomic DNA using the primers TCGGATCCATGAATCTCAATGAAAGC and ATGAATTCCCTGTCACAAGTTAAAACAC. The PCR fragment was cleaved with *Bam*HI and *Eco*RI and cloned into the corresponding sites of the N-terminal GFP-fusion vector pUG36 (Guldener and Hegemann, http://mips.gsf.de/proj/yeast/info/tools/hegemann/gfp.html) to create pGFPMON1. BY4742 cells were transformed with pUG36 and pGFPMON1. Transformants incubated on SC solid media, depleted of methionine to induce the *MET25* promoter, were immobilized in 0.7% agarose. Images were obtained with a Zeiss Axiovision 2.05 microscope, using a Plan NeoFluar 40×/0.75 objective equipped with a DIC or FITC filter.

3. Results

3.1. Mon1p is essential for maturation of proaminopeptidase I

In the yeast deletion project a collection of ∼5000 deletion strains, each deleted for a single open reading frame, was generated. This collection covers the non-essential part of the yeast genome, corresponding to ∼85% of the whole genome. We previously screened this deletion collection for strains with a reduced ability to survive during nitrogen starvation, a characteristic but not unique phenotype of autophagy mutants [24]. Since this quite pleiotropic assay identified over 1000 strains, we further checked these 1000 strains for defects in proaminopeptidase I maturation, which indicate a more specific defect in autophagy. We here report detection of *mon1Δ* cells in this screen. For further characterization we chromosomally deleted *MON1* in the WCG4a background with a PCR-generated cassette conferring kanamycin resistance (see Section 2.2). Gene replacement was confirmed by Southern (not shown).

In non-starved cells, where the cvt-pathway is active, no mature proaminopeptidase I was detectable (Fig. 1, lane 4), whereas the enzyme is fully processed in wild-type cells due to the active cvt-pathway (Fig. 1, lane 3). Furthermore, starvation for extended times (up to 24 h), which induced autophagy in wild-type cells, did not overcome the proaminopeptidase I maturation defect in *mon1Δ* cells (Fig. 1, lanes 5 and 6). Since maturation of proaminopeptidase I requires mature vacuolar proteinase B [25], we checked for the presence of mature proteinase B in *mon1Δ* cells. Consistent with the previously described vacuolar protein sorting defects [2], we found that non-starved *mon1Δ* cells contain some proproteinase B (Fig. 1, lane 4); however, enough mature proteinase B is present (Fig. 1, lanes 4–6). Taken together, this suggests an essential function for Mon1p in the cvt-pathway and autophagy.

3.2. Quantitative analysis of autophagy in mon1Δ cells

To quantify the autophagic defect of *mon1Δ* cells, we used the Pho8Δ60-assay established by Noda et al. [22]. Alkaline

Table 1

Strain	Genotype	Reference
WCG4a	*Mat α his3-11,15 leu2-3 ura3*	[15]
YKMW2	WCG4a *Mat α mon1Δ::KAN^R*	this study
YKMW7	WCG4a *Mat α ccz1Δ::KAN^R*	[16]
YKMW10	WCG4a *Mat a ypt7Δ::HIS3*	[16]
YKMW20	WCG4a *Mat α ccz1Δ:: KAN^R pho8Δ::LEU2*	this study
YKMW22	WCG4a *Mat α mon1Δ:: KAN^R pho8Δ::LEU2*	this study
YUE63	WCG4a *Mat α pho8Δ::LEU2*	this study
YUE66	WCG4a *Mat α aut5Δ:: KAN^R pho8Δ::LEU2*	this study
YIS4	WCG4a *Mat α aut5Δ::KAN^R*	[11]
YMS30	WCG4a *Mat a aut3Δ:: KAN^R*	[17]
YMTA	WCG4a *Mat a; his3-11,15 leu2-3 ura3 pep4Δ::HIS3*	[15]
BY4742	*Matα his3Δ1 leu2Δ0 lys2Δ0 ura3Δ0*	Euroscarf, Frankfurt, Germany
BY4743	*Mat a/α his3Δ1/his3Δ;1 leu2Δ0/leu2Δ0 lys2Δ0/LYS2 MET15/met15Δ0 ura3Δ0/ura3Δ0*	Euroscarf, Frankfurt, Germany
DYY101	*MATα leu2-3,112 ura3-52 his3-Δ200 trp1-Δ901 ade2-101 suc2-Δ9 ape1::LEU2*	[18]

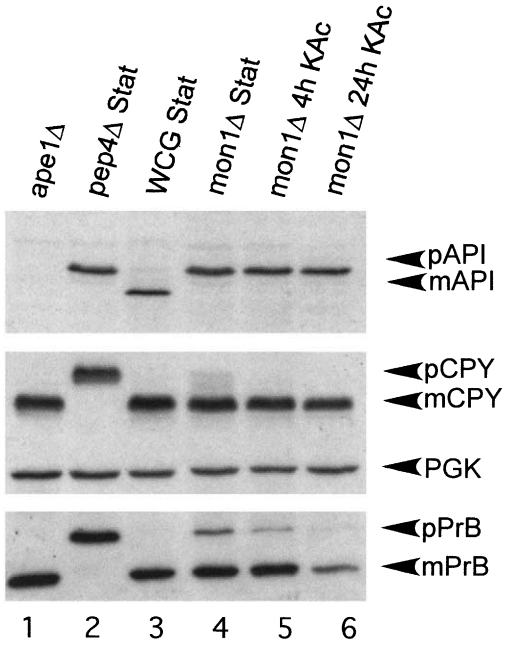

Fig. 1. Proaminopeptidase I maturation is defective in starved and non-starved *mon1*Δ cells. Crude extracts of stationary phase cells (stat) or cells starved for the indicated times in 1% K-acetate were immunoblotted and analyzed with antibodies against proaminopeptidase I (API) (upper panel); CPY and PGK (middle); proteinase B (PrB) (lower panel). p: proform; m: mature. Wild-type (WCG), proteinase A deficient (*pep4*Δ) and proaminopeptidase I deficient cells (*ape1*Δ) were included as controls.

phosphatase (Pho8p) is synthesized as an inactive precursor, which is targeted to the vacuole, and then activated proteolytically. In Pho8Δ60p the ER import sequence is deleted, the truncated enzymatically inactive protein therefore accumulates in the cytosol. After starvation induction of autophagy Pho8Δ60p is transported to the vacuole and activated. Alkaline phosphatase activity therefore quantitatively corresponds to the autophagic capacity [22]. For this assay, we chromosomally deleted *PHO8* in the strains used and expressed Pho8Δ60p from a plasmid (see Section 2.4). As shown in Fig. 2A, autophagy is almost completely blocked in *mon1*Δ cells, similar to *aut5*Δ cells, which are defective in intravacuolar lysis of autophagic bodies [11,10].

Homozygous diploid autophagy mutants typically are defective in the cell differentiation process of sporulation [3]. Indeed homozygous diploid *mon1*Δ cells are unable to form asci (Fig. 2B).

3.3. *Autophagy is impaired in mon1Δ cells prior to vacuolar fusion of autophagosomes*

We next wished to determine at which step autophagy is affected in *mon1*Δ cells. When yeast cells are starved for nitrogen in the presence of the proteinase B inhibitor PMSF, autophagic bodies accumulate in the vacuoles [8]. These vesicles can be visualized in light microscopy. We detected no autophagic bodies within the fragmented vacuoles of *mon1*Δ cells under these conditions (Fig. 3A). However, the fragmented vacuoles might interfere with detection of autophagic bodies. We therefore further used a GFP-Aut7 fusion protein as a visible marker for cvt-vesicles and autophagosomes [5,6]. Aut7p is involved in the biogenesis of these vesicles and during their formation it is specifically enclosed within their lumen. In non-starved wild-type cells, GFP-Aut7p is clearly detectable at the dot-like preautophagosomal structure proximal to the vacuole (Fig. 3B). In starved wild-type cells, it is transported to the vacuole inside autophagosomes, where their breakdown release quite proteolysis-resistant GFP (Fig. 3B). As shown in fluorescence microscopy of starved and non-starved *mon1*Δ cells, GFP-Aut7p did not enter the vacuoles but accumulated in multiple dot-like structures outside the vacuoles (Fig. 3B). This strongly suggests a block of the autophagic pathway before vacuolar fusion of cvt-vesicles and autophagosomes. Since GFP-Aut7p is degraded inside the vacuole, resulting in formation of free GFP, we additionally analyzed GFP-Aut7p degradation in immunoblots to monitor autophagy. Consistent with microscopy and the quantitative evaluation of autophagy using Pho8Δ60p, almost no free GFP was detectable in *mon1*Δ cells (Fig. 3C). To indicate the es-

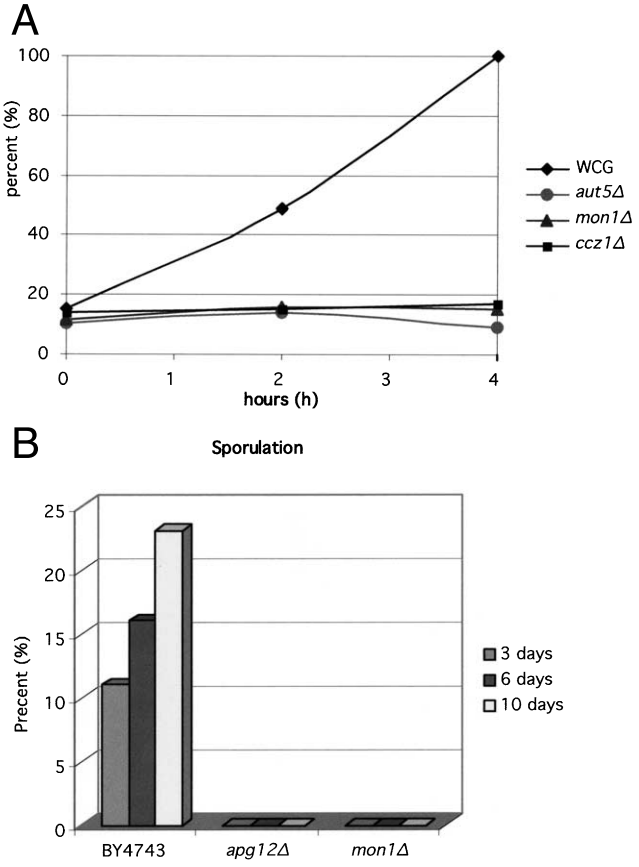

Fig. 2. Autophagy is blocked in *mon1*Δ cells. A: Quantitative measurement of autophagy in *mon1Δ pho8*Δ cells expressing Pho8Δ60p from a plasmid. In wild-type cells, enzymatically inactive Pho8Δ60p is transported via autophagy to the vacuole and proteolytically activated. At the indicated times aliquots of cells starving in nitrogen-free SD–N medium are withdrawn and enzymatic activity is measured (see Section 2.4). Enzymatic activity in wild-type (WCG) cells after 4 h starvation was set to 100%. *aut5*Δ and *ccz1*Δ cells, which are defective in autophagy, are included. Further details in the text. B: Homozygous diploid *mon1*Δ cells are unable to sporulate. Cells were incubated in 1% K-acetate at room temperature and at the indicated times the combined number of tetrads and dyads were counted and expressed as a percentage of total cells.

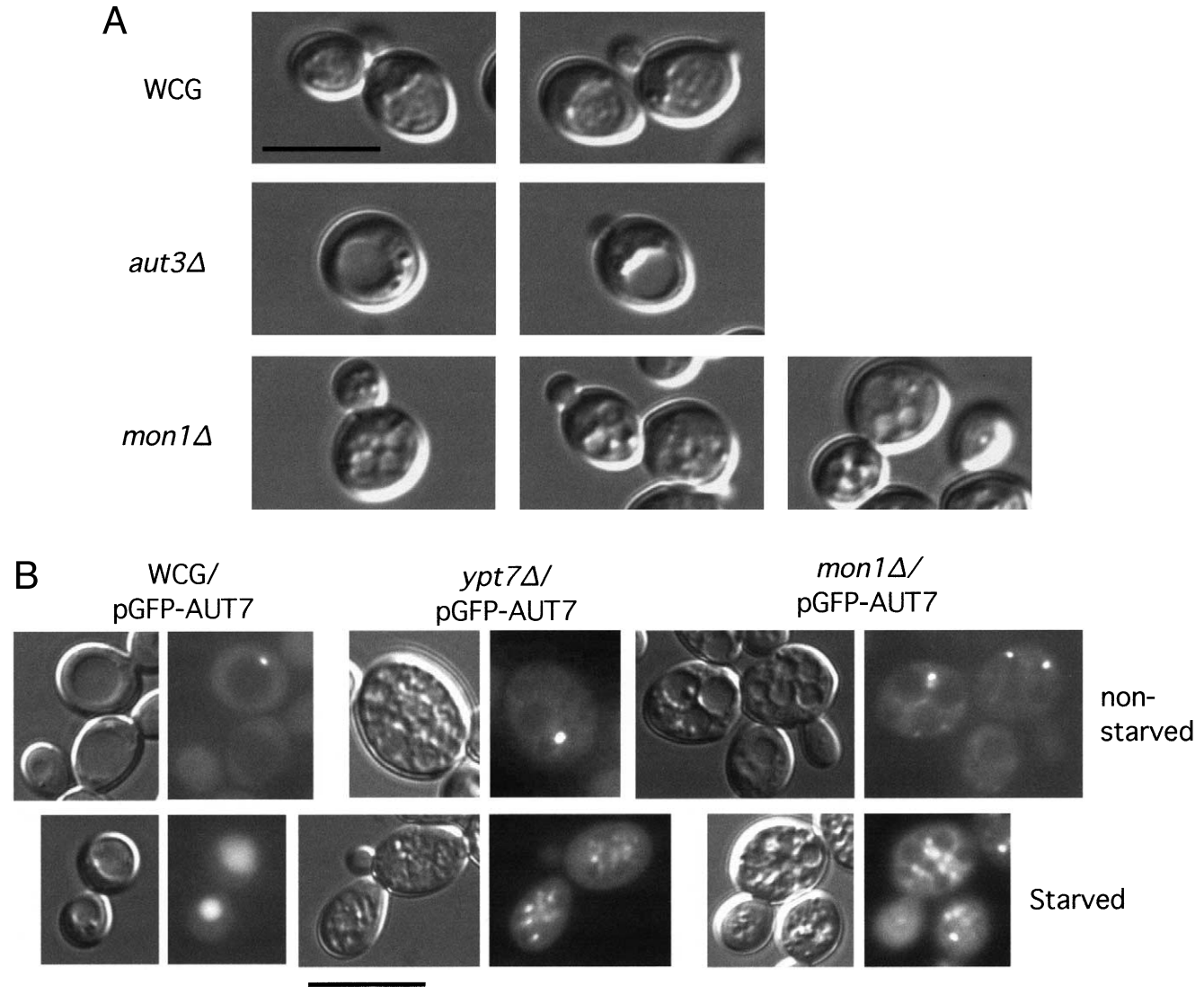

Fig. 3. The autophagic block in *mon1*Δ cells occurs before vacuolar uptake of autophagosomes. A: *mon1*Δ cells were starved for 4 h in nitrogen-free SD–N medium with the proteinase B inhibitor PMSF. Wild-type (WCG) and *aut3*Δ cells defective in autophagy were included. Bar: 10 μm. B: The autophagosomal marker GFP-Aut7p accumulate in non-starved (upper panel) and starved (4 h in SD–N, lower panel) *mon1*Δ cells at punctate structures outside the vacuole. Cells expressing GFP-Aut7p from a centromeric plasmid with its native promotor were analyzed in fluorescence microscopy. Wild-type (WCG) and *ypt7*Δ cells exhibiting a defect in vacuolar uptake of autophagosomes were included. Bar: 10 μm. C: The autophagosomal marker GFP-Aut7p is not degraded in *mon1*Δ cells. Cells expressing GFP-Aut7p from a centromeric plasmid with its endogenous promotor were shifted to nitrogen starvation medium (SD–N). At the indicated times, aliquots were taken and immunoblotted with antibodies against GFP, which detects both GFP-Aut7 and free GFP (upper row) and cytosolic PGK (lower row) as a loading control. Wild-type (WCG), *ypt7*Δ, *aut10*Δ cells expressing GFP-Aut7p and wild-type cells without GFP-Aut7p (WCG) were included. *ypt7*Δ and *aut10*Δ cells are defective in autophagy.

sential function of Mon1p in autophagy, we termed it Aut12p, but will further use the official name Mon1p.

3.4. Proaminopeptidase I accumulates in membrane-protected form in *mon1*Δ cells

To further dissect, at which step the cvt-pathway and autophagy are impaired in *mon1*Δ cells, we checked whether proaminopeptidase I, another specific cargo of cvt-vesicles and autophagosomes, accumulates in protease-accessible or membrane-protected form. We used non-starved *mon1*Δ cells to check the effect on the cvt-pathway (Fig. 4A) and cells starved for nitrogen to evaluate autophagy (Fig. 4B). Under both conditions, treatment of hypotonically lysed spheroplasted *mon1*Δ cells with proteinase K did not result in degradation of proaminopeptidase I (Fig. 4A and B, lane 5). Treatment with proteinase K together with the detergent Triton X-100, however, led to degradation of proaminopeptidase I (Fig. 4A and B, lane 6). As controls, we included *apg1*Δ (*aut3*Δ) cells, impaired in formation of cvt-vesicles and autophagosomes, and *ypt7*Δ cells, defective in vacuolar fusion of these vesicles. To exclude that membrane protection is mimicked by unlysed cells, we additionally separated the hypotonically lysed spheroplasts in a 10 000 × *g* pellet (Fig. 4A and B, lane 2) and supernatant (Fig. 4A and B, lane 3). The lack of cytosolic PGK in the pellet fractions confirms the absence of contaminating whole cells. These findings show that in *mon1*Δ cells cvt-vesicles and autophagosomes are still formed but are unable to fuse with the vacuole.

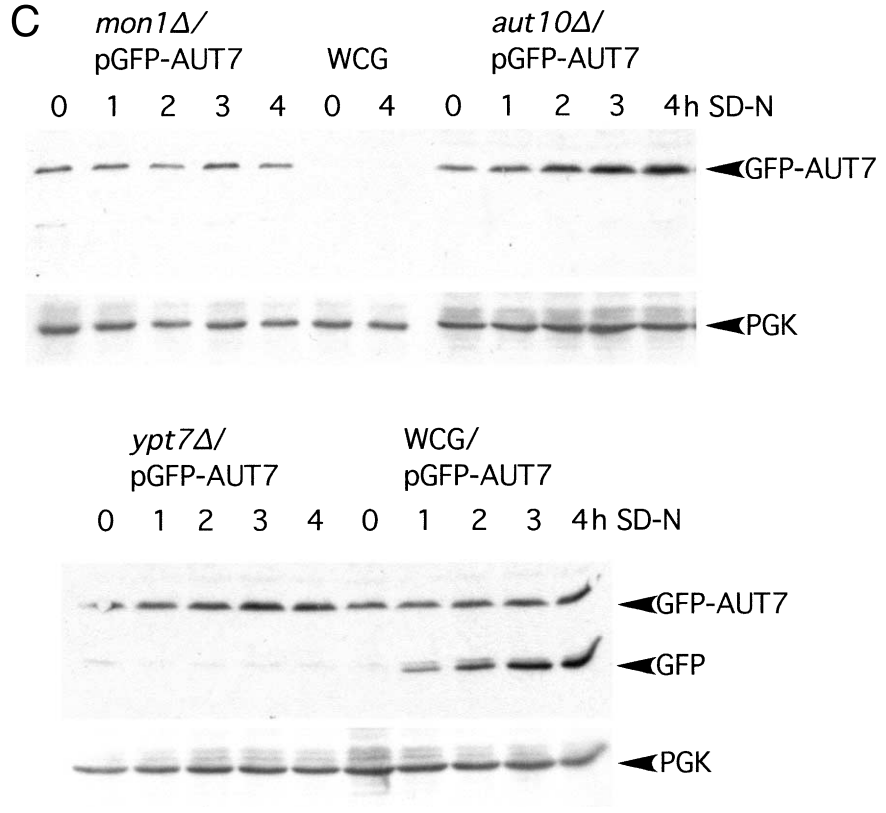

Fig. 3 (*Continued*).

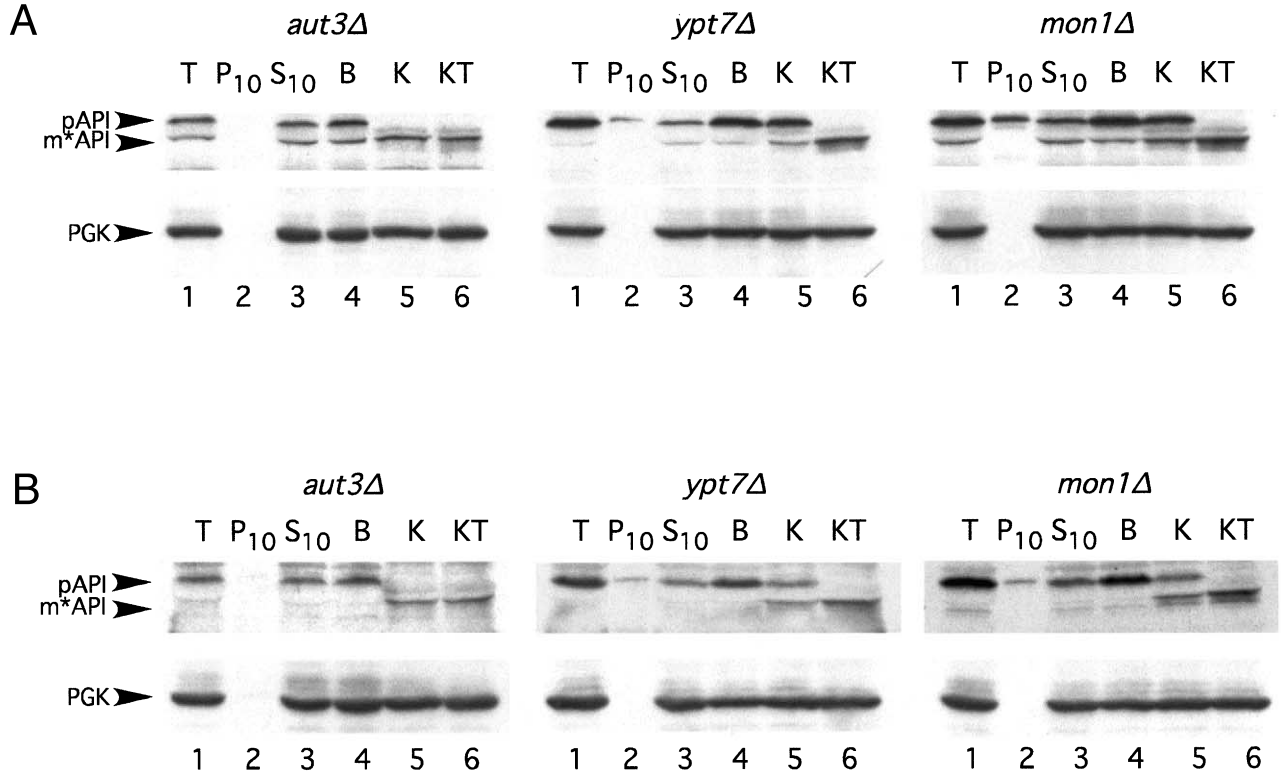

Fig. 4. In non-starved (A) and 4 h in SD–N starved (B) *mon1*Δ cells proaminopeptidase I is proteinase-protected. Hypotonically lysed spheroplasts were treated with buffer (B, lane 4), proteinase K (K, lane 5) and proteinase K+Triton X-100 (KT, lane 6). The samples were then immunoblotted with antibodies against proaminopeptidase I (upper panel). An aliquot of the spheroplast lysate was further centrifuged at $10\,000 \times g$ and separated into a P_{10} pellet and a S_{10} supernatant fraction. Immunoblotting with antibodies against cytosolic PGK confirmed the absence of contaminating whole cells. Note that proaminopeptidase I is not degraded by proteinase K but converted into a mature-like form marked as m*API.

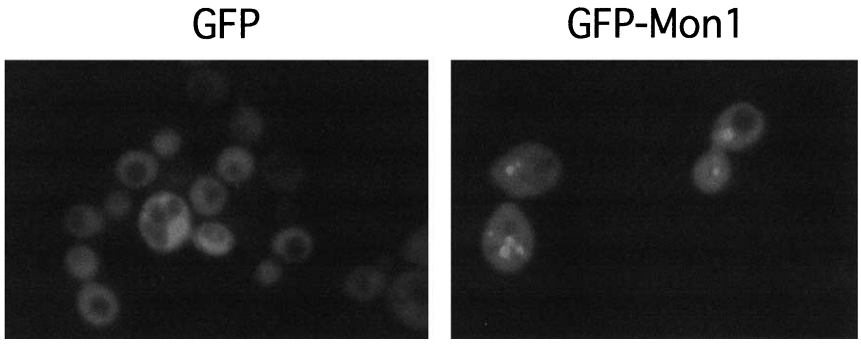

Fig. 5. GFP-Mon1p localizes to the cytosol and to cytosolic punctated structures. Wild-type cells expressing GFP (left) or GFP-Mon1p were grown in methionine-free medium and analyzed by fluorescence microscopy.

3.5. *Mon1-GFP is located in the cytosol and at cytosolic, punctate structures*

To learn more about the intracellular localization of Mon1p, we generated a plasmid-encoded Mon1-GFP fusion protein under control of the methionine-regulated *MET25*-promotor (see Section 2.7). Most interestingly, fluorescence microscopy showed beside a cytosolic localization the presence of punctate structures in the cytosol (Fig. 5). This would be compatible with the recruitment of Mon1p to some membranes, as expected for a function in vacuolar fusion of cvt-vesicles and autophagosomes.

4. Discussion

Our findings clearly demonstrate an essential function of Mon1p in the cvt-pathway and autophagy, supported by the following. (i) Proaminopeptidase I maturation is blocked in non-starved and starved *mon1*Δ cells, even after prolonged starvation (Fig. 1). (ii) Homozygous diploid *mon1*Δ cells are unable to sporulate, which is typical for autophagy mutants (Fig. 2B). (iii) Most convincingly, a quantitative evaluation of autophagy in starving *mon1*Δ cells showed a complete block (Fig. 2A). Several explanations could be responsible for the observed block of autophagy and the cvt-pathway. First of all, proteins might still reach the vacuolar lumen but, due to the lack of mature vacuolar proteinases or due to another defect in lysing autophagic bodies, their intravacuolar breakdown might be inhibited. We therefore confirmed that in *mon1*Δ cells despite their kinetic defect in vacuolar protein sorting, significant steady-state levels of mature vacuolar proteinase B are present (Fig. 1). We further used GFP-Aut7p, which is specifically enclosed in cvt-vesicles and autophagosomes, as a tool to directly monitor the autophagic protein transport in fluorescence microscopy. The accumulation of GFP-Aut7p at punctate structures outside the vacuoles and the lack of vacuolar fluorescence (Fig. 3B) in *mon1*Δ cells clearly demonstrates a block before vacuolar uptake of autophagosomes and cvt-vesicles. This is further confirmed by immunoblots (Fig. 3C) and the lack of intravacuolar autophagic bodies in *mon1*Δ cells, starved in the presence of the proteinase B inhibitor PMSF (Fig. 3A). This suggests a function of Mon1p either in biogenesis of proaminopeptidase I-containing vesicles or in their vacuolar fusion. Defects in biogenesis of vesicles result in cytosolic accumulation of proaminopeptidase I in proteinase K accessible form, while a defect in vacuolar fusion of the vesicles leads to the accumulation of proaminopeptidase I trapped inside these vesicles. Our experiments with starved and non-starved *mon1*Δ cells revealed proteinase protection of proaminopeptidase I (Fig. 4A and B). This suggests a function of Mon1p in the fusion of cvt-vesicles and autophagosomes with the vacuolar membrane. Furthermore, recruitment of GFP-Mon1p to cytosolic punctate structures (Fig. 5) fits well with such a function. Based on our data, we speculate that Mon1p has a similar function in the vacuolar protein-sorting pathway. Proteins sharing homology with Mon1p are present in species from *Anopheles gambiae* to *Homo sapiens*, our study might therefore be useful in studying these proteins. Ypt7p and Ccz1p [16,26,27] are also involved in vacuolar fusion of cvt-vesicles and autophagosomes. It will therefore be interesting to see if there are functional interactions between Mon1p and these proteins.

Acknowledgements: We are grateful to Y. Ohsumi, P.E. Thorsness, J. Hegemann and S.F. Nothwehr for plasmids, to the people of the deletion project and to D.H. Wolf and U.D. Epple for support. This work was supported by the 'Deutsche Forschungsgemeinschaft', the 'Fonds der Chemischen Industrie' to M.T. and from the 'Swedish Cancer Society' and the 'Erik and Mai Pehrsson Foundation' to H.R.

References

[1] Muren, E., Oyen, M., Barmark, G. and Ronne, H. (2001) Yeast 18, 163–172.
[2] Bonangelino, C.J., Chavez, E.M. and Bonifacino, J.S. (2002) Mol. Biol. Cell 13, 2486–2501.
[3] Thumm, M. (2000) Microsc. Res. Tech. 51, 563–572.
[4] Klionsky, D.J. and Ohsumi, Y. (1999) Annu. Rev. Cell Dev. Biol. 15, 1–32.
[5] Suzuki, K., Kirisako, T., Kamada, Y., Mizushima, N., Noda, T. and Ohsumi, Y. (2001) EMBO J. 20, 5971–5981.
[6] Kim, J., Huang, W.P., Stromhaug, P.E. and Klionsky, D.J. (2001) J. Biol. Chem. 277, 763–773.
[7] Noda, T., Suzuki, K. and Ohsumi, Y. (2002) Trends Cell Biol. 12, 231–235.
[8] Takeshige, K., Baba, M., Tsuboi, S., Noda, T. and Ohsumi, Y. (1992) J. Cell Biol. 119, 301–311.
[9] Suriapranata, I., Epple, U.D., Bernreuther, D., Bredschneider, M., Sovarasteanu, K. and Thumm, M. (2000) J. Cell Sci. 113, 4025–4033.
[10] Teter, S.A., Eggerton, K.P., Scott, S.V., Kim, J., Fischer, A.M. and Klionsky, D.J. (2001) J. Biol. Chem. 276, 2083–2087.
[11] Epple, U.D., Suriapranata, I., Eskelinen, E.L. and Thumm, M. (2001) J. Bacteriol. 183, 5942–5955.
[12] Baba, M., Osumi, M., Scott, S.V., Klionsky, D.J. and Ohsumi, Y. (1997) J. Cell Biol. 139, 1687–1695.
[13] Ausubel, F.M., Brent, R., Kingston, R.E. and Moore, D.D.

(1987) Current Protocols in Molecular Biology, Greene Publishing Associates, New York, NY.
[14] Barth, H. and Thumm, M. (2001) Gene 274, 151–156.
[15] Thumm, M., Egner, R., Koch, B., Schlumpberger, M., Straub, M., Veenhuis, M. and Wolf, D.H. (1994) FEBS Lett. 349, 275–280.
[16] Meiling-Wesse, K., Barth, H. and Thumm, M. (2002) FEBS Lett. 526, 71–76.
[17] Straub, M., Bredschneider, M. and Thumm, M. (1997) J. Bacteriol. 179, 3875–3883.
[18] Klionsky, D.J., Cueva, R. and Yaver, D.S. (1992) J. Cell Biol. 119, 287–299.
[19] Güldener, U., Heck, S., Fielder, T., Beinhauer, J. and Hegemann, J.H. (1996) Nucleic Acids Res. 24, 2519–2524.
[20] Nothwehr, S.F., Conibear, E. and Stevens, T.H. (1995) J. Cell Biol. 129, 35–46.
[21] Campbell, C.L. and Thorsness, P.E. (1998) J. Cell Sci. 111, 2455–2464.
[22] Noda, T., Matsuura, A., Wada, Y. and Ohsumi, Y. (1995) Biochem. Biophys. Res. Commun. 210, 126–132.
[23] Scott, S.V., Guan, J., Hutchins, M.U., Kim, J. and Klionsky, D.J. (2001) Mol. Cell 7, 1131–1141.
[24] Barth, H., Meiling-Wesse, K., Epple, U.D. and Thumm, M. (2001) FEBS Lett. 508, 23–28.
[25] Harding, T.M., Morano, K.A., Scott, S.V. and Klionsky, D.J. (1995) J. Cell Biol. 131, 591–602.
[26] Kucharczyk, R., Kierzek, A.M., Slonimski, P.P. and Rytka, J. (2001) J. Cell Sci. 114, 3137–3145.
[27] Kucharczyk, R., Dupre, S., Avaro, S., Haguenauer-Tsapis, R., Slonimski, P.P. and Rytka, J. (2000) J. Cell Sci. 113 Pt. 23, 4301–4311.